

sign of ( $\chi_{\parallel}$ - $\chi_{\perp}$ ) for aziridines.

In summary, values of ( $\chi_{\parallel}$ - $\chi_{\perp}$ ) for the SiW<sub>11</sub>Co complexes of aziridine derivatives have been found to be positive by analysis of the isotropic NMR shifts, while that for the SiW<sub>11</sub>Co complexes of pyridine derivatives is negative. This result indicates that the ordering of  $d_{xy}$  and  $d_{xz}$ ,  $d_{yz}$  orbitals in SiW<sub>11</sub>Co complexes can be reversed by ligands.

**Acknowledgment.** Financial support of the Ministry of Education (BSRI-95-3411) is gratefully acknowledged.

### References

- Ko, M.; Rhyu, G. I.; So, H. *Bull. Korean Chem. Soc.* **1993**, *14*, 500.
- Ko, M.; Rhyu, G. I.; So, H. *Bull. Korean Chem. Soc.* **1994**, *15*, 673.
- Woo, H. Y.; Kim, J. Y.; So, H. *Bull. Korean Chem. Soc.* **1995**, *16*, 1176.
- Woo, H. Y.; So, H.; Pope, M. T. *J. Am. Chem. Soc.* **1996**, *118*, 621.
- Happe, J. A.; Ward, R. L. *J. Chem. Phys.* **1963**, *39*, 1211.
- Dermer, O. C.; Ham, G. E. *Ethylenimine and Other Aziridines*, Academic Press: New York, 1969; p 94.
- Morishima, I.; Yonezawa, T. *J. Chem. Phys.* **1971**, *54*, 3238.
- Simmons, V. E. Ph.D. Thesis, Boston University (1963).
- Weakley, T. J. R.; Malik, S. A. *J. Inorg. Nucl. Chem.* **1967**, *29*, 2935.
- Buckles, R. E.; Mock, G. V. *J. Am. Chem. Soc.* **1948**, *70*, 1275.
- Bertini, I.; Canti, G.; Luchinat, C.; Mani, F. *J. Am. Chem. Soc.* **1981**, *103*, 7784.
- Koenig, S. H. *J. Magn. Reson.* **1978**, *97*, 2113.
- Mortimer, F. S. *J. Mol. Spectry.* **1960**, *5*, 199.
- Elleman, D. D.; Manatt, S. L.; Pearce, C. D. *J. Chem. Phys.* **1965**, *42*, 650.
- The NMR spectrum was simulated by using the computer program NMRS developed by Dr. H. M. Bell of Virginia Polytechnic Institute and State University, and downloaded from <http://www.chem.vt.edu/simulation/VTNMR.html>.
- Kluiber, R. W.; Horrocks, W. D., Jr. *J. Am. Chem. Soc.* **1965**, *87*, 5350.
- Kim, J. Y.; Park, S. M.; So, H. *Bull. Korean Chem. Soc.* **1997**, *18*, 369.
- Bak, B.; Skaarup, S. *J. Mol. Struct.* **1971**, *10*, 385.
- Elder, R. C. *Inorg. Chem.* **1968**, *7*, 1117.
- The same Co-N distance was used for all three complexes. The least mean square difference may be reduced slightly, if the Co-N distance is varied.
- Dean, J. A. *Handbook of Organic Chemistry*; McGraw-Hill: New York, 1987.
- Safo, M. K.; Gupta, G. P.; Watson, C. T.; Simonis, U.; Walker, F. A.; Scheidt, W. R. *J. Am. Chem. Soc.* **1992**, *114*, 7066.

## Analysis of Complex Forced Rayleigh Scattering Decay Profiles for the Diffusion of Methyl Yellow in Binary Solution

Ha Seon Park, Jungmoon Sung<sup>†</sup>, Hyunjung Lee, Taihyun Chang\*, and Daniel R. Spiegel<sup>‡</sup>

*Department of Chemistry, POSTECH, Pohang 790-784, Korea*

<sup>‡</sup>*Department of Physics, Trinity University, San Antonio, TX 78212-7200 USA*

*Received June 12, 1997*

The nature and analysis methods of complicated decay profiles found in forced Rayleigh scattering (FRS) have been investigated for the probe diffusion of methyl yellow in 2-propanol. The complementary shifted and ground state grating effect, which is known to be the origin of non-single exponential decays, was analyzed by non-linear regression fitting to a double exponential model function. We confirmed that the parameters were highly correlated so that it was difficult to extract a unique set of parameters in the presence of experimental noise. Nevertheless, a reasonable range of decay time constants could be estimated from the grating spacing dependence.

### Introduction

Recently the forced Rayleigh scattering (FRS) technique has been widely used for the study of mass diffusion in various media.<sup>1-10</sup> The technique measures the decay of the light intensity diffracted from a periodic concentration grat-

ing created by the illumination of an optical fringe pattern within a sample containing an appropriate photoprobe. In order for the concentration grating to diffract light, the photo-reaction product (shifted state) must possess different optical properties from the unshifted state either in absorptivity (amplitude grating) or in refractive index (phase grating), or both.<sup>11-14</sup> If the transient sinusoidal concentration profile decays with a single relaxation time constant, the diffracted

<sup>†</sup>Current address: Taedok Institute of Technology, Yukong Ltd.

optical field decays exponentially and the diffracted light intensity is

$$I_d = [A \exp(-t/\tau) + B_{coh}]^2 + B_{inc} \quad (1)$$

where  $\tau$ ,  $B_{coh}$  and  $B_{inc}$  are the decay time constant, coherent background and incoherent background, respectively. The decay time constant  $\tau$  is a function of the probe diffusivity and the shifted state lifetime so that information on the dynamics of the photoprobe can be obtained. If the photoprobe is bound to a macromolecule of interest, one can obtain the diffusivity of the macromolecule.<sup>1-3,7,8</sup>

However, deviations from single exponential decays have often been observed; such deviation is ascribed to the difference in the diffusivities of the optically shifted and unshifted state photoprobe.<sup>5,6,9,14</sup> Under these circumstances, the time-varying diffracted intensity has been analyzed by the following model function,

$$I_d(t) = [A_1 \exp(-t/\tau_1) - A_2 \exp(-t/\tau_2) + B_{coh}]^2 + B_{inc} \quad (2)$$

where  $\tau_1$  and  $\tau_2$  are the respective decay time constants of two complementary gratings, and  $A_1$  and  $A_2$  represent the amplitudes of the optical fields diffracted from each complementary grating. If the two decay time constants are identical, the single exponential decay of eq. 1 is obtained. If two decay time constants are different, the decay profile departs from a single exponential to two limits, growth-decay (GD, for the case of  $\tau_1/\tau_2 > A_1/A_2 > 1$  or  $\tau_1/\tau_2 < A_1/A_2 < 1$ ) and decay-growth-decay (DGD, for the case of  $A_1 > A_2$ ,  $\tau_1 < \tau_2$  or  $A_1 < A_2$ ,  $\tau_1 > \tau_2$ ) signal.<sup>14,15</sup>

With inherent noise existing in the decay signal, it is difficult to find a unique set of A's and  $\tau$ 's from a nonlinear regression curve fitting to eq. 2 since the parameters are highly correlated.<sup>6,14-17</sup> Recognizing the difficulties inherent in the nonlinear fitting methods, Park *et al.*<sup>16</sup> and Spiegel *et al.*<sup>15</sup> proposed methods to obtain the mean decay time constants from nonmonotonic decays, although these methods cannot provide fully satisfactory solutions. Meanwhile, fitting to the double exponential model function has been pursued with little attention to possible pitfalls, and we feel that a more critical evaluation of the analysis method is desirable. In this work, we selected simple dye/solvent binary systems (methyl yellow in toluene and 2-propanol) displaying a single exponential and DGD signal, respectively. We experimentally removed a parameter,  $B_{coh}$  in eq. 2, so that we could more critically evaluate and compare different data-reduction methods for FRS signals. In so doing, we hope not only to shed light on the diffusivity of an important FRS photochrome, but also on the difficulties inherent in the analysis of complex FRS profiles.

## Experimental

The probe dye, 4-dimethylaminoazobenzene (methyl yellow; MY) and the analytical grade solvents, toluene and 2-propanol were acquired from Aldrich and used without further purification. The solutions of MY were prepared at a concentration of 0.1 mg/mL and filtered through 0.2  $\mu$ m pore PTFE membrane filter (Gelman) directly to a 5 mm path length spectroscopic quartz cuvette for the FRS measurements. The temperature of the cell was controlled at  $25.0 \pm 0.1$  °C.

The FRS apparatus previously described in detail<sup>9</sup> was modified by inserting a half wave plate (CVI laser) into the path of one of the two writing beams for every other pulse during the accumulation of the FRS signal in order to eliminate the coherent baseline contribution. The half wave plate shifts the grating phase by  $\pi$  at every other pulse while the phase of the coherent baseline remains unchanged. As a result, after an even number of accumulations, one obtains the decay signal as follows.

$$I_d(t) = [A \exp(-t/\tau)]^2 + B_{inc} \quad (3)$$

or

$$I_d(t) = [A_1 \exp(-t/\tau_1) - A_2 \exp(-t/\tau_2)]^2 + B_{inc} \quad (4)$$

The schematic diagram of the modified instrument is shown in Figure 1. We found that this method works well and is much simpler than other methods previously reported.<sup>13,18</sup>

The analysis scheme chosen for the decay profiles depended on the shape of the signal. For single exponential decay signals, a nonlinear regression fit to eq. 1 or eq. 3 was used. The results from the fit to eq. 1 and 3 were identical, confirming the efficient elimination of the  $B_{coh}$  with the half wave plate. For the DGD profiles, the average decay time constant was determined by the  $\Delta t$  method ( $\Delta t = t_{max} - t_{min}$ , i.e., the time lapse between the dip and maximum position).<sup>16</sup> Then the diffusivity of MY is obtained from the slope of  $1/\tau$  (or  $1/\Delta t$ ) vs.  $q^2$  plot according to the following relationship,

$$1/\tau \text{ (or } 1/\Delta t) = Dq^2 + 1/\tau_{life} \quad (5)$$

where  $\tau_{life}$  is the lifetime of the shifted state,  $q = 2\pi/d$ , and  $d$  is the spacing of the optical fringe pattern created by the writing pulse. The spacing of the optical fringe pattern is calculated from the crossing angle of the writing beams according to  $d = \lambda/[2\sin(\theta/2)]$  where  $\lambda$  and  $\theta$  are the wavelength and the crossing angle of the writing beams, respectively. We also attempted to obtain two individual decay time constants in eq. 4 by a nonlinear regression fitting method.

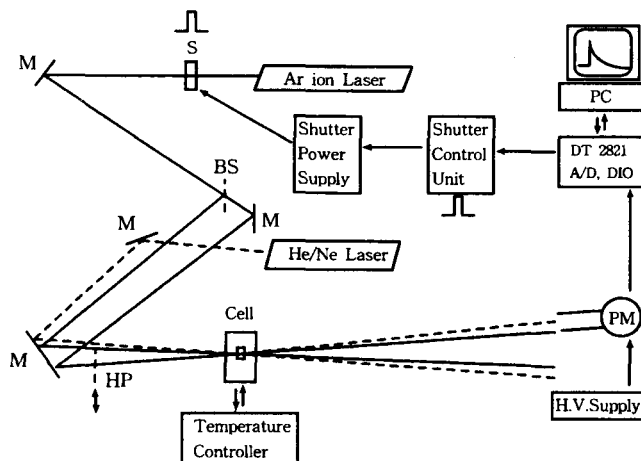


**Figure 1.** Schematic diagram of the FRS apparatus used in this study. S: electronic shutter, BS: beam splitter, M: mirrors, HP: half wave plate, PM: photomultiplier tube.

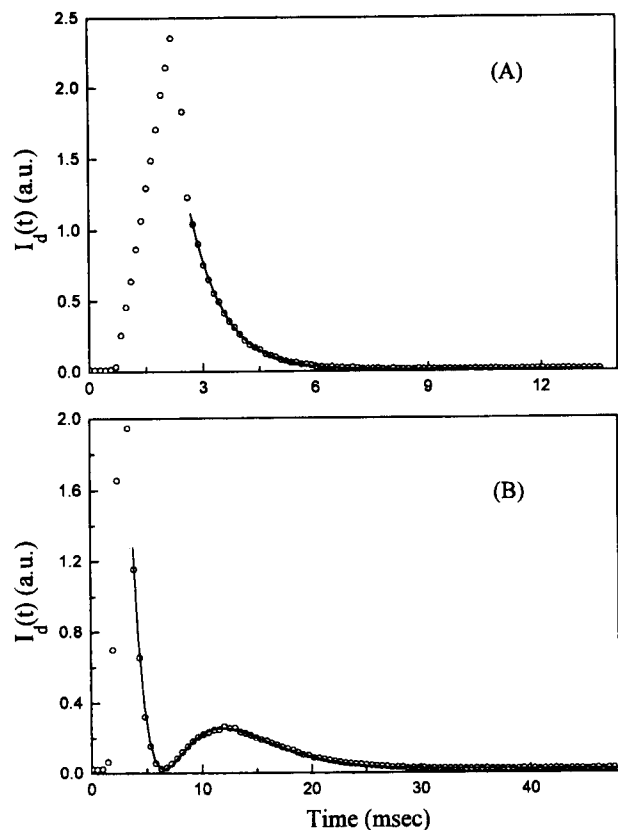


**Figure 2.** FRS decay profiles of MY in toluene (A) and in 2-propanol (B) at the same crossing angle of the writing beam,  $2.79^\circ$ . The solid lines drawn in the plots (A) and (B) are the best fit according to the model functions of eq. 3 and eq. 4, respectively.

## Results and Discussion

**Solvent dependence of FRS decay signal.** Figure 2 shows the FRS decay profiles of MY in toluene (A) and in 2-propanol (B) at the same writing beam crossing angle. The decay profiles in the two solvents are distinctively different. The decay profile in toluene shows a clean single exponential decay following the fast thermal grating decay,<sup>18</sup> while a typical DGD profile is observed in the 2-propanol medium. The solid lines drawn in the plot (A) and (B) are the best fits according to the model functions of eq. 3, and eq. 4, respectively. The fitting to eq. 3 in (A) is found to be unique and we can get a single decay time constant. A semi-logarithmic plot (not shown) of the data in Figure 2(A) is linear as the signal changes by nearly three powers of ten, demonstrating that a single-exponential approach is appropriate. On the other hand, the fitting to eq. 4 strongly depends on the initial guess of the parameters and a unique fit was not realized. We will come back to this in more detail later. The decay time constant in toluene is obtained by fitting to eq. 3 while the  $\Delta t$  method is used for the 2-propanol solution. The  $q^2$  dependence of  $1/\tau$  and  $1/\Delta t$  according to eq. 5 is shown in Figure 3. As shown in the figure, an excellent  $q^2$  dependence is found in both solvents and the diffusivities of MY from the  $q^2$  dependence are  $1.4 \times 10^{-5}$  cm<sup>2</sup>/s and  $4.6 \times 10^{-6}$  cm<sup>2</sup>/s in toluene and 2-propanol, respectively. From the Stokes-Einstein relationship,  $D = kT/(6\pi\eta R)$ ,

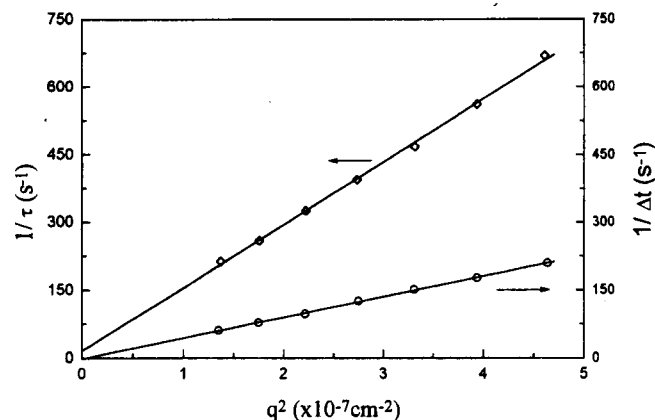


**Figure 3.** Grating spacing dependence of  $1/\tau$  ( $\diamond$ , in toluene) and  $1/\Delta t$  ( $\circ$ , in 2-propanol) at  $25^\circ\text{C}$ . Both show excellent  $q^2$  dependences. From the slope of the plots (eq. 5), diffusivities of MY are obtained in toluene and in 2-propanol as  $1.40 \times 10^{-5}$  cm<sup>2</sup>/s and  $4.57 \times 10^{-6}$  cm<sup>2</sup>/s, respectively.

we obtain the Stokes radius of the dye as  $2.8 \pm 0.2$  Å and  $2.4 \pm 0.1$  Å in toluene and 2-propanol, respectively. The agreement, while reasonable, is slightly outside the experimental uncertainty, which is calculated from the 95% confidence limit of the Student's  $t$ -distribution. Since it is rather well established that the diffusivity is not inversely proportional to the solvent viscosity when the molecular sizes of the diffusant and solvent are comparable, this result is not very surprising.<sup>19</sup> More extensive work on the relationship between small-molecule diffusivity and medium viscosity is being carried out in this laboratory.

On the other hand, we do not at the moment have a rigorous quantitative explanation for why MY shows different decay profiles in two solvents. Deviation from single-exponential decays has been observed by others with a different azo dye, methyl red, although the DGD profile was not as evident as for methyl yellow.<sup>20,21</sup> We suspect that the solvent polarity is responsible for the different decay profiles since the DGD profile is observed in many alcoholic solvents such as methanol, ethanol, etc, while single exponential decay is observed in hydrophobic solvents such as toluene, hexane, and CCl<sub>4</sub>. It is likely that the dipole moment of *cis* MY induces stronger solvation of the molecule in alcoholic solvents, which leads to a slower diffusion than *trans* MY, with its smaller dipole moment. Since the refractive index of the *cis* form is known to be smaller than the *trans* form of azobenzene derivatives, the slower diffusion of *cis* MY results in the DGD type signal.<sup>6,14,16</sup> A detailed study on this issue is in progress and will be reported elsewhere later.

### Extraction of individual decay time constants.

Our next question concerns whether we can extract the two individual decay time constants of the complementary gratings. Difficulties in obtaining a unique set of  $A$ 's and  $\tau$ 's, due to the high correlation between the parameters, have been previously reported.<sup>6,14,16,17</sup> However these early conclusions were made without the benefit of more recent advances in the FRS method; for example, most of the works used eq. 4 for the data fitting without elimination of the coherent baseline. In our laboratory, we have repeatedly ob-

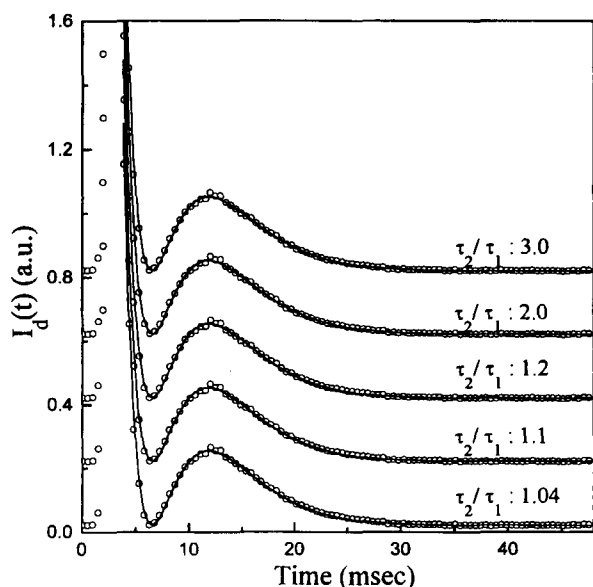


**Figure 4.** Five different non-linear regression fit results of an DGD type profile of MY in 2-propanol shown in Figure 2 (B). The solid lines represent the fit results according to eq. 4 with different initial input of  $\tau_1$  and  $\tau_2$  for the nonlinear regression. The numbers in the figure denote the initial input of  $\tau_2/\tau_1$  while the each set of initial  $\tau_1$  and  $\tau_2$  was chosen to have the same  $(\tau_1\tau_2)^{1/2} (= \Delta t)$  value. The final fit results are nearly identical with the initial input when  $\tau_2/\tau_1$  is not too large (as summarized in Table 1), and the quality of the fits is hard to distinguish.

served that even a small  $B_{coh}$  makes a significant difference in the final result. The addition of an extra parameter also makes a nonlinear regression fit result much less reproducible. Therefore we remove a parameter,  $B_{coh}$ , using a half wave plate as described above. Nonetheless, we found that it was still very difficult to find a unique set of 5 parameters from the non-linear regression fit. This is elaborated in Figure 4, where the five different fits of an FRS profile using different sets of initial guesses for  $\tau_1$  and  $\tau_2$  are displayed. The experimental decay profile is the one shown in Figure 2(B) and the numbers on the plot represent the value of  $\tau_2/\tau_1$  used for the initial guess. The initial sets of  $\tau_1$  and  $\tau_2$  were chosen to have the same  $(\tau_1\tau_2)^{1/2} (= \Delta t)$  value.<sup>16</sup> A typical nonlinear regression routine by the unscaled Marquardt algorithm was used, and the quality of the fits are hard to distinguish from one another with the existing noise. The final values of A's and  $\tau$ 's are found to be very sensitive to the initial guess of the non-linear regression routine as shown in Table 1. When we take initial  $\tau_1$  and  $\tau_2$  values which differ by less than 20%, we obtain the final fit results with  $\tau_1$  and  $\tau_2$  close to the initial guess. In other words, eq. 4 can fit the experimental profile well by adjusting  $A_1$  and  $A_2$  without modifying  $\tau_1$  and  $\tau_2$  much. Therefore the final  $\tau_1$  and  $\tau_2$  obtained from the fit as in Figure 4 are not exactly equal but very similar to their respective initial input values. On the other hand, there seems to be an upper limit such that the value of  $\tau_2/\tau_1$  does not exceed a factor of *ca.* 2 for a much larger initial input of  $\tau_2/\tau_1$ . In any event, the decay profile itself can be fitted nicely to the model function, eq. 4 as shown in Figure 4. Therefore, it does not seem possible to extract individual diffusivities

**Table 1.** Initial Guess vs. Final Fit Result of Figure 3

Initial Input*				Final result			
$\tau_1$	$\tau_2$	$\tau_2/\tau_1$	$(\tau_1\tau_2)^{1/2}$	$\tau_1$	$\tau_2$	$\tau_2/\tau_1$	$(\tau_1\tau_2)^{1/2}$
5.54	5.76	1.04	5.65	5.22	5.41	1.04	5.31
5.37	5.93	1.1	5.64	5.08	5.56	1.09	5.31
5.08	6.22	1.2	5.62	4.85	5.84	1.20	5.32
3.95	8.07	2.0	5.65	4.28	6.74	1.57	5.37
3.25	9.83	3.0	5.65	4.20	6.89	1.64	5.38

\*Initial guess was made from  $\Delta t = t_{max} - t_{min} = 5.65$  msec.

of the two MY isomers unless we know the A's in eq. 4, which could be experimentally determined,<sup>12</sup> but has never been seriously attempted for mass diffusion studies. We believe that the extraction of  $\tau_1$  and  $\tau_2$  individually remains an unresolved problem in the FRS technique and must be approached with proper caution. On the other hand,  $(\tau_1\tau_2)^{1/2} (= \Delta t)$  value remains practically the same regardless of the input and final set of  $\tau_1$  and  $\tau_2$ , which is expected from the  $\Delta t$  analysis scheme.<sup>16</sup>

For the next step, the  $q^2$  dependence of the four sets of decay time constants obtained through the above mentioned procedure is examined as displayed in Figure 5. In the figure we show the diffusivities obtained from the slopes together with the initial input values of  $\tau_2/\tau_1$  for the nonlinear regression fit. We can see that the  $q^2$  dependence starts to deviate from eq. 5 as the initial input value of  $\tau_2/\tau_1$  exceeds *ca.* 1.2. If we employ the  $q^2$  dependence as an additional criterion for a successful fit, we are able to claim that the diffusivities of the trans and the cis form of methyl yellow in 2-propanol differ by no more than 15%. In any event, the geometric mean of two diffusivities  $D_1$  and  $D_2$  are in good agreement with the value obtained by the  $\Delta t$  method,  $4.6 \times 10^{-6}$  cm<sup>2</sup>/s.

In summary, we found that methyl yellow in pure sol-

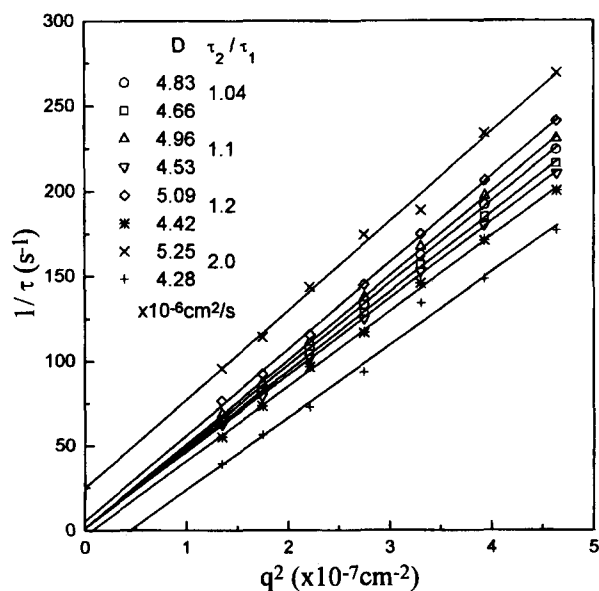


**Figure 5.** Grating spacing dependence of  $\tau_1$  and  $\tau_2$  determined by fit to eq. 4 using different initial guesses for  $\tau_2/\tau_1$ .  $1/\tau_1$  and  $1/\tau_2$  show a good  $q^2$  dependence when they are not very different each other.

vents could exhibit a nonmonotonic FRS decay profile. Consideration of permanent dipole moments and the polarity of the solvent provides a qualitative explanation for this observation although a more systematic study appears to be necessary to understand the behavior in detail. We also confirmed experimentally that the extraction of two individual diffusivities from DGD type FRS decay profiles is very troublesome. Nonetheless, we can measure the mean diffusivity quite reliably, and we can at least infer a range for  $\tau_1$  and  $\tau_2$  individually from the  $q^2$  dependence of the  $\tau$ 's. Difficulty in deducing individual  $\tau$ 's from nonmonotonic FRS decay signals seems to be inherent to FRS method, which evidently mandates independent measurements of the amplitudes  $A_1$  and  $A_2$ .

**Acknowledgment.** This work was supported in part by a grant from the Korea Ministry of Education (BSRI-95-3438).

### References

- Hervet, H.; Leger, L.; Rondelez, F. *Phys. Rev. Lett.* **1979**, *42*, 1861.
- Kim, H.; Chang, T.; Yohanan, J. M.; Wang, L.; Yu, H. *Macromolecules* **1986**, *19*, 2737.
- Rhee, K. W.; Gabriel, D. A.; Johnson Jr., C. S. *J. Phys. Chem.* **1984**, *88*, 4010.
- Antonietti, M.; Coutandin, J.; Grutter, R.; Sillescu, H. *Macromolecules* **1984**, *17*, 798.
- Zhang, J.; Wang, C. H. *J. Phys. Chem.* **1986**, *90*, 2296.
- Huang, W. J.; Frick, T. S.; Landry, M. R.; Lee, J. A.; Lodge, T. P.; Tirrel, M. *AIChE J.* **1987**, *33*, 573.
- Tran-Cong, Q.; Chang, T.; Han, C. C.; Nishijima, Y. *Polymer* **1988**, *29*, 2261.
- Nemoto, N.; Kishine, M.; Inoue, T.; Osaki, K. *Macromolecules* **1990**, *23*, 659.
- Lee, J.; Park, T.; Sung, J.; Park, S.; Chang, T. *Bull. Korean Chem. Soc.* **1991**, *12*, 596.
- Park, H. S.; Sung, J.; Chang, T. *Macromolecules* **1996**, *29*, 3216.
- Kogelnik, H. *Bell Syst. Tech. J.* **1969**, *48*, 2909.
- Nelson, K. A.; Casalegno, R.; Miller, R. J. D.; Fayer, M. D. *J. Chem. Phys.* **1982**, *77*, 1144.
- Johnson Jr., C. S. *J. Opt. Soc. Am. B.* **1985**, *2*, 317.
- Park, S.; Sung, J.; Kim, H.; Chang, T. *J. Phys. Chem.* **1991**, *95*, 7121.
- Spiegel, D. R.; Sprinkle, M. B.; Chang, T. *J. Chem. Phys.* **1996**, *104*, 4920.
- Park, S.; Yu, H.; Chang, T. *Macromolecules* **1993**, *26*, 3086.
- Lee, J. A.; Lodge, T. P. *J. Phys. Chem.* **1987**, *91*, 5546.
- Köhler, W. *J. Chem. Phys.* **1993**, *98*, 660.
- Hayduk, W.; Cheng, S. C. *Chem. Eng. Sci.* **1971**, *26*, 635.
- Lee, S. H.; Kim, S. K. *Bull. Korean Chem. Soc.* **1996**, *17*, 365.
- Terazima, M.; Okamoto, K.; Hirota, N. *J. Chem. Phys.* **1993**, *97*, 5188.

## Structure-Reactivity Relationship of Substituted Phenylethyl Arenesulfonates with Substituted Pyridines under High Pressure

Heon-Young Park, Ki-Joo Son, Duck-Young Cheong, and Soo-Dong Yoh\*

*Department of Chemistry, Teacher's College, Kyungpook National University, Taegu 702-701, Korea*

*Received June 15, 1997*

Nucleophilic substitution reactions of (Z)-phenylethyl (X)-benzenesulfonates with (Y)-pyridines were investigated in acetonitrile at 60 °C under respective pressures. The magnitudes of the Hammett reaction constants,  $\rho_X$ ,  $\rho_Y$  and  $\rho_Z$  indicate that a stronger nucleophile leads to a greater degree of bond formation of C-N and a better leaving group is accompanied by a less degree of bond breaking. The magnitude of correlation interaction term,  $\rho_{ij}$  can be used to determine the structure of the transition state (TS) for the  $S_N$  reaction. As the pressure is increased, the Hammett reaction constants,  $\rho_X$  and  $|\rho_Y|$ , are decreased, but correlation interaction coefficient,  $\rho_{XZ}$  and  $|\rho_{YZ}|$ , are increased. The results indicate that the reaction of (Z)-phenylethyl (X)-benzenesulfonates with (Y)-pyridines probably moves from a dissociative  $S_N2$  to early-type concerted  $S_N2$  mechanism by increasing pressure. This result shows that the correlation interaction term  $\rho_{ij}$  can be useful tool to determine the structure of TS, and also the sign of the product  $\rho_{XZ} \cdot \rho_{YZ}$  can be predict the movement of the TS.

### Introduction

One of the linear free energy relationships (LFER), the notable Hammett equation, has been used as an empirical means of characterizing transition-state (TS) structures.<sup>1-3</sup> The Hammett  $\rho$  is first derivative of  $\log k$  as shown in

equation (1) and reflects TS structures involved in a series of reactions with structural changes affecting the reaction center.

$$\rho = \log k / \partial \sigma \quad (1)$$

The magnitudes of the  $\rho$  values in the nucleophile and